LUND UNIVERSITY

Impact of current localization on the performance of compact MIMO antennas

Li, Hui; Lau, Buon Kiong; Tan, Yi; He, Sailing; Ying, Zhinong

LUND UNIVERSITY

PO Box 117
221 00 Lund
+46 46-222 00 00

H. Li, B. K. Lau, Y. Tan, S. He, and Z. Ying, "Impact of current localization on the performance of compact MIMO antennas," in *Proc. 5th Europ. Conf, Antennas Propagat. (EuCAP'2011)*, Rome, Italy, Apr. 11-15, 2011.

Impact of Current Localization on the Performance of Compact MIMO Antennas

H. Li[1,2], B. K. Lau[1], Y. Tan[1], S. He[2], and Z. Ying[3]

[1] Department of Electrical and Information Technology, Lund University, SE-221 00 Lund, Sweden.
{Hui.Li, Buon_Kiong.Lau, Yi.Tan}@eit.lth.se
[2] School of Electromagnetic Engineering, Royal Institute of Technology, S-100 44 Stockholm, Sweden
Sailing.He@ee.kth.se
[3] Corporate Technology Office, Sony Ericsson Mobile Communications AB, SE-221 88 Lund, Sweden.
Ying.Zhinong@sonyericsson.com

Abstract—In this paper, we study the influence of current localization on the isolation between two antennas in a compact terminal setting. The two antennas are chosen to be a monopole and a PIFA. The degree of current localization is controlled by the permittivity value of the PIFA's dielectric loading. Both lossless and lossy cases are simulated in order to ascertain the underlying performance impact from current localization and its potential use in real implementation. Our results show that significant isolation enhancement is achieved with more localized currents. Moreover, the technique improves the terminal's diversity and capacity performance both at the center frequency and over a given bandwidth. In addition, PIFAs with dielectric loadings of higher permittivity values and more localized currents are physically smaller. Antenna prototypes are fabricated, and the measured results agree well with the simulated results.

I. INTRODUCTION

Multiple-input multiple-output (MIMO) is an important enabling technology for high throughput data transmission in both existing and upcoming wireless communication systems. The key advantage of MIMO is its potential to linearly increase channel capacity with the number of antennas at both the transmitter and receiver, without sacrificing additional frequency spectrum and transmit power [1]. In reality, some applications such as mobile terminals may require antennas to be closely spaced, which result in strong mutual coupling and a degradation in the expected capacity gain. Recent results indicate that the MIMO performance of closely spaced antennas can be improved through decoupling methods [2], including decoupling networks [3], neutralization line [4], quarter wavelength filter [5], and additional local ground plane [6]. The main purpose of some of these techniques (e.g., [5], [6]) is to localize the current of the antenna into a small area and thus prevent it from flowing along the shared ground plane. However, mutual coupling is influenced by many factors, such as radiation pattern, antenna polarization and the ground plane current distribution; and thus it is difficult to distinguish ground plane coupling from over-the-air coupling.

This paper analyzes the trade-off in the MIMO antenna performance of dual-antenna terminal prototypes for different degrees of current localization on one antenna. In order to isolate the effect of current localization on the ground plane from other factors that can also influence MIMO performance, the degree of localization is controlled by varying the permittivity of the dielectric loading of the antenna. Here, the current localization analysis is performed in a mobile terminal setting. This is because a compact mobile terminal can be viewed as the worst case scenario with respect to coupling, since the ground plane (chassis) is used as a shared radiator at low mobile frequency band (e.g. at 850 MHz), and the current along it is very strong [7]. Through current localization, the chassis mode will be less excited by the current localized antenna, and the MIMO performance can be improved.

In Section II, simulation results for the trade-off analysis of MIMO performance assuming lossless materials (i.e., ideal conditions) are presented. In Section III, the same simulations are performed under lossy condition in order to study the practicality of the current localization technique. Prototypes are made, and measured results are given in Section IV, followed by some conclusions in Section V.

II. ANTENNAS WITH LOSSLESS MATERIALS

A. Antenna Geometry

The dimensions of the chassis used in our work are 100 mm × 40 mm, which correspond to the typical size of a candybar-type mobile phone. It consists of a 0.1 mm copper layer on a 1.55 mm FR4 substrate with relative permittivity (ε_r) of 4.7 and loss tangent of 0.015. A (slot) monopole and a PIFA, two of the most commonly used antenna types in today's mobile phones, are implemented on the chassis. The geometry and the parameters of the antenna system are shown in Fig. 1. The slot monopole is etched into the ground plane on the substrate of FR4, and fed by a microstrip line (i.e., the dashed line in Fig. 1) on the other side of the substrate. The width of both of the slots is $W_S = 5$ mm.

To exclude other factors which can also influence the MIMO performance, the basic structure of the antenna of interest (i.e., PIFA) should be unchanged. Different levels of

current localization of the PIFA are realized by only varying the relative permittivity values of the dielectric loading. Three monopole-and-PIFA prototypes are designed, and the relative permittivity values of the dielectric loadings for the PIFAs are 1 (i.e., no dielectric loading, which corresponds to Fig. 1 with an electrically neutral substrate for PIFA), 6 and 20, respectively. To keep the resonant frequency of the PIFA constant, the antenna with a high permittivity dielectric loading should be a miniaturized and proportional copy of the one with a lower permittivity dielectric loading. However, the height of the PIFA is unchanged for all three cases. A scale-down factor (SF), which describes the degree of lateral miniaturization, is defined as follows

$$\text{SF} = \frac{\text{the area of the miniaturized antenna}}{\text{the area of the original antenna}} \quad (1)$$

The SFs for the three PIFAs are 1, 0.47 and 0.2116, respectively, where the PIFA in Fig. 1 is the no-loading case.

The antennas are analyzed under both lossless and lossy conditions. The purpose of lossless case is to obtain an upper bound of achievable MIMO performance improvement from current localization, since only mismatch and mutual coupling are considered. To investigate the more practical case, the lossy condition is also studied. In our study, the focus is on the effect of current localization on MIMO performance, and thus no attempt is made to optimize the antenna bandwidth.
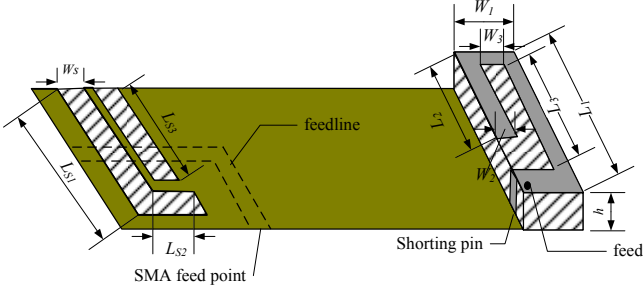

Fig.1. Geometries of the slot monopole and the PIFA. The dimensions are: L_{S1} = 39 mm, L_{S2} = 6 mm, L_{S3} = 24mm, W_S = 5 mm, L_1 = 40 mm, L_2 = 26.2 mm, L_3 = 28 mm, W_1 = 17 mm, W_2 = 4 mm, W_3 = 8 mm, h = 6 mm.

B. Antenna Performance with Lossless Materials

Antennas with lossless materials are studied first (i.e., all ohmic losses are excluded), since antennas of different sizes have different radiation efficiencies for the same material loss tangent. Thus, only mismatch and mutual coupling are considered in this case.

Full-wave antenna simulations are carried out in the frequency domain using the CST Microwave Studio software. The center frequency of the PIFA is chosen to be at 0.94 GHz, and both antennas are well matched (S_{11}, S_{22} < -10 dB) at this frequency. The normalized current distributions of the simulated prototypes when the PIFAs are excited (and the monopoles terminated in 50 Ω) are shown in Fig. 2. Since the chassis works as a radiator, it is unavoidable that there is current flowing along the chassis. However, as the relative permittivity increases, the current along the chassis decreases, and it becomes more localized around the PIFA.
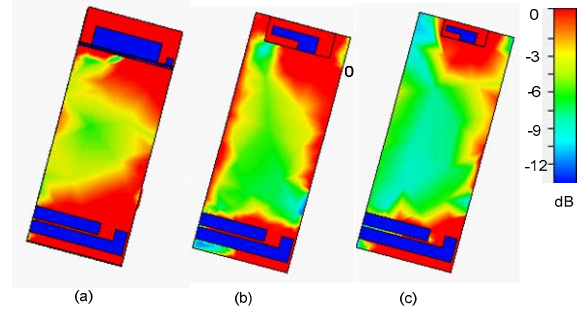

Fig. 2. Normalized magnitude of current distributions for PIFA with: (a) ε_r = 1, (b) ε_r = 6, (c) ε_r = 20

TABLE I ANTENNA PERFORMANCE (LOSSLESS)

		$\varepsilon_r = 1$	$\varepsilon_r = 6$	$\varepsilon_r = 20$
S_{21} at f_c (dB)		-2.5	-3.5	-4.3
η_{total} at f_c	PIFA	40.4%	52.6%	55.0%
	monopole	34.2%	52.5%	55.3%
Bandwidth of PIFA (MHz)		23.2	14.2	8
Correlation at f_c		0.57	0.6	0.55
Capacity with EP (bits/s/Hz)	at f_c	5.92	7.35	7.8
	10 MHz	5.90	7.22	7.25
	20 MHz	5.84	7.05	7.1
EDG with MRC (dB)	at f_c	6.46	7.66	8.21
	10 MHz	6.38	7.43	7.61
	20 MHz	6.26	7.17	7.28

The simulation results are presented in Table I, including the coupling coefficient (S_{21}), the total efficiency (η_{total}) and the correlation at the center frequency (f_c), the 6 dB impedance bandwidth of the PIFA, as well as the capacity and diversity performance over different bandwidths of 0 MHz (at f_c), 10 MHz and 20 MHz. The bandwidth of the monopole is not shown in the table because it is large enough to cover the bandwidths of interest. The effective diversity gain (EDG) is calculated with maximum ratio combining (MRC), taken at 1% probability. The channel capacity with equal power (EP) allocation is calculated for the reference signal-to-noise ratio (SNR) of 20 dB. The Kronecker channel model and uniform 3D angular power spectrum (APS) are assumed. There is no correlation between the (base station) transmit antennas, whereas the (mobile terminal) receive antennas are correlated according to their radiation patterns and the 3D APS. The capacity is averaged over 10,000 i.i.d. Rayleigh realizations of the channel at each frequency. The channels are normalized with respect to the i.i.d. Rayleigh case, which means that the correlation, total efficiency and power imbalance (efficiency imbalance) are taken into account in the capacity evaluation. In addition, the capacity and EDG are averaged over a given bandwidth (i.e., 10 MHz and 20 MHz) to give a fair comparison between antennas of different dielectric loadings. This is because a higher permittivity dielectric loading leads to a physically smaller antenna, which changes its bandwidth. The maximum bandwidth of 20 MHz is based on the maximum bandwidth for one physical channel in Long Term Evolution (LTE) (assuming that adaptive matching may be

applied to the PIFA to cover the entire receive band). The capacity with water-filling power allocation is not shown in the table due to its similar trend as that with EP allocation.

From Table I, several conclusions can be made: When the current distribution of the PIFA becomes more localized, i.e., the relative permittivity increases from 1 to 20,

1) The efficiencies of the PIFA and monopole increase. Since both antennas are well matched, this improvement is mainly attributed to the reduced mutual coupling;
2) The bandwidth of the PIFA greatly decreases from 23 MHz to 8 MHz. This is because when the dimensions of the PIFA are reduced, the Q factor increases, and the Q factor is inversely proportional to the bandwidth;
3) The correlation between the antennas, as calculated from the far field pattern, does not change appreciably, which illustrates that the polarization and the radiation patterns (over-the-air coupling factors) are almost constant;
4) Though the impedance bandwidth is reduced, the capacity with EP and EDG over 20 MHz still increase by 1.26 bits/s/Hz and 1 dB, respectively. The advantage becomes more obvious if they are calculated over a narrower bandwidth, due to narrowband behaviour of the PIFAs with higher permittivity dielectric loadings.

It can be concluded from the simulation results of antennas with lossless materials that the current localization of the PIFA not only reduce the implementation space on the chassis (due to the PIFA being physically smaller), the technique can also improve MIMO performance within a certain bandwidth.

III. ANTENNAS WITH LOSSY MATERIALS

To analyse the three dual-antenna prototypes more practically, all material losses are now considered. The loss tangent of the PIFA's dielectric loading is 0.01 for all cases. The loss tangent of the chassis' FR-4 substrate is 0.015. The conductivity of the copper is 5.8×10^7 S/m. The simulated scattering parameters with the dielectric loading $\varepsilon_r = 1$ and 20 are shown in Fig. 3. It is observed that the isolation improves by 5 dB when ε_r increases from 1 to 20.

The performance metrics given in Table I for the lossless condition are likewise obtained for the corresponding lossy condition (see Table II). The trends observed in Table I are also seen in Table II; however, several differences are noted:

1) When the PIFA becomes more localized, the total efficiency of the PIFA is greatly reduced due to its smaller radiation efficiency, which is given by

$$\eta_{rad} = \frac{R_r}{R_r + R_L},$$
(2)

where R_r is the radiation resistance and R_L represents the conduction-dielectric (ohmic) losses;

2) When compared to the lossless case, the bandwidth of the PIFA increases regardless of the permittivity, due to ohmic loss. The isolation improvement from increasing the permittivity value also becomes more obvious than in the lossless case, which can be attributed to the lower efficiency of the PIFA;
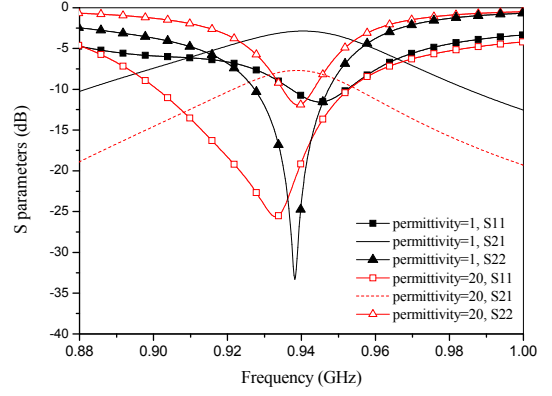

Fig. 3. The scattering (or S) parameters for the PIFA-monopole prototypes, with the PIFA's dielectric loadings of $\varepsilon_r = 1$ and 20 in the lossy condition.

TABLE II ANTENNA PERFORMANCE (LOSSY)

		$\varepsilon_r = 1$	$\varepsilon_r = 6$	$\varepsilon_r = 20$
S_{21} at f_c (dB)		-2.9	-5.5	-8
η_{total} of antennas	PIFA	41.6%	25.4%	18.4%
	monopole	30.9%	63%	73.9%
Bandwidth of PIFA		36.3	26.8	20.6
Correlation at f_c		0.64	0.74	0.70
Capacity under EP (bits/s/Hz)	at f_c	5.72	6.22	6.33
	10 MHz	5.67	6.22	6.32
	20 MHz	5.61	6.2	6.28
EDG with MRC (dB)	at f_c	6.04	6.08	6.07
	10 MHz	5.93	5.95	5.87
	20 MHz	5.83	5.84	5.72

3) The improvements in capacity are less obvious than those in Table I and slight degradations in diversity gains are seen with increasing localization, since the efficiencies of both antennas drop.

Another issue that should be noted is that the same loss tangent is used here for fair comparison. In reality, the assumed loss tangent of 0.01 is quite high for a dielectric material with $\varepsilon_r = 20$. If real materials of lower ohmic losses are used, the performance improvement due to current localization is closer to the (lossless) upper bounds in Table I.

Moreover, although ohmic loss can have a negative impact on the MIMO performance (i.e., diversity gain) of the cases with a more localized antenna, the localized antenna is still beneficial from the viewpoint of antenna miniaturization.

IV. EXPERIMENTS AND DISCUSSIONS

The three simulated PIFA-monopole prototypes are fabricated and shown in Fig. 4. For dielectric loading with $\varepsilon_r = 20$, a ceramic material is used. It has a loss tangent of 0.001, which is less than that used in the simulation. All three cases are measured, and the measured results agree well with the simulations. Due to space constraint, only one case is presented in this paper, i.e., PIFA with dielectric permittivity of 6. The scattering parameters are measured with a vector

network analyzer, and shown in Fig. 5, together with the simulation results. The bandwidths of both the monopole and PIFA are a little larger than those in the simulations, because of cable loss and fabrication tolerance. For the same reasons, the measured isolation is also better than the simulated one.

The far field electric field patterns are measured in a Satimo Stargate-64 antenna measurement facility. The patterns at the center frequency are shown in Fig. 6. The slight differences between the measured patterns and the simulated ones are caused by the influences of the feeding cables.

V. CONCLUSIONS

In this study, the impact of antenna current localization on MIMO performance is examined through simulations with both lossless and the lossy materials. By varying the permittivity of the PIFA's dielectric loading, the effect of current localization on coupling (and MIMO performance) can be studied independently of other contributing factors. Antenna performances, including bandwidth, total efficiency, correlation, diversity and channel capacity, are analyzed. It is concluded that antenna localization can be beneficial both in terms of antenna miniaturization and improved MIMO performance. Antenna prototypes are fabricated and measured. The measured results agree well with the simulations.
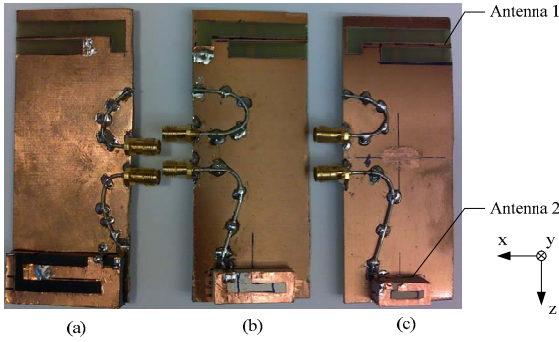

Fig. 4 Dual-antenna prototypes, where the PIFA's dielectric loadings have the permittivity values of (a) $\varepsilon_r = 1$, (b) $\varepsilon_r = 6$, (c) $\varepsilon_r = 20$.
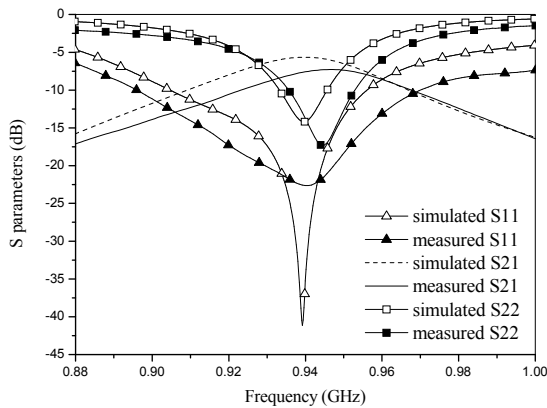

Fig. 5 Simulated and measured scattering parameters of the dual-antenna prototype, for the case of PIFA with $\varepsilon_r = 6$, see Fig. 4(b).
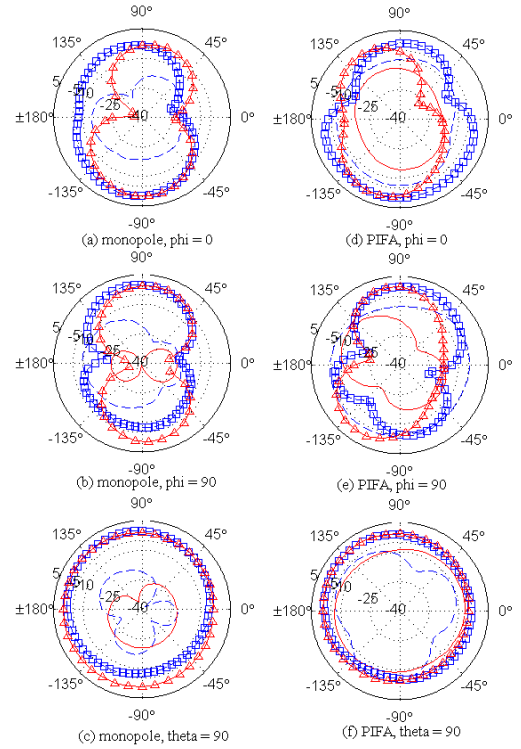

Fig. 6 Simulated and measured antenna patterns for the dual-antenna prototype, when the dielectric loading of the PIFA has the permittivity value of $\varepsilon_r = 6$. (——) simulated E(Phi), (– –) measured E(Phi), (–△–) simulated E(Theta), (–□–) measured E(Theta).

REFERENCES

[1] M. A. Jensen and J. W. Wallace, "A review of antennas and propagation for MIMO wireless communications," *IEEE Trans. On Antennas and Propagat.,* vol. 52, no. 11, pp. 2810-2824, Nov. 2004.

[2] B. K. Lau, "Multiple antenna terminals," in *MIMO: From Theory to Implementation*, C. Oestges, A. Sibille, and A. Zanella, Eds. San Diego: Academic Press, 2011, pp. 267-298.

[3] B. K. Lau, J. B. Andersen, G. Kristensson, and A. F. Molisch, "Impact of matching network on bandwidth of compact antenna arrays," *IEEE Trans. Antennas Propagat.*, vol. 54, no. 11, pp. 3225-3238, Nov. 2006.

[4] A. Diallo, C. Luxey, P. L. Thuc, R. Staraj, and G. Kossiavas, "Enhanced two-antenna structures for universal mobile telecommunications system diversity terminals," *IET Microw. Antennas Propogat.,* vol. 2, no. 1, pp. 93-101, 2008.

[5] H. Li, J. Xiong, and S. He, "A compact planar MIMO antenna system of four Elements with similar radiation characteristics and isolation structure," *IEEE Antennas Wireless Propagat. Lett.,* vol. 8, pp. 1107-1110, 2009.

[6] Y. Gao, X. Chen, Z. Ying, and C. Parini, "Design and performance investigation of a dual-element PIFA array at 2.5GHz for MIMO terminal," *IEEE Trans. Antennas Propag.,* vol. 55, no.12, pp. 3433-3441, Dec. 2007.

[7] V. Plicanic, B. K. Lau, A. Derneryd, and Z. Ying, "Actual diversity performance of a multiband diversity antenna with hand and head effects," *IEEE Trans. Antennas Propagat.,* vol. 57, no. 5, pp. 1547-1556, May. 2009.